Open access • Posted Content • DOI:10.1101/2020.06.26.173203

Population Bottlenecks and Intra-host Evolution during Human-to-Human Transmission of SARS-CoV-2Population Bottlenecks and Intra-host Evolution during Human-to-Human Transmission of SARS-CoV-2 — Source link

Daxi Wang, Yungui Wang, Wanying Sun, Lei Zhang ...+26 more authors

Published on: 26 Jun 2020 - bioRxiv

Topics: Viral replication

Related papers:

- Population Bottlenecks and Intra-host Evolution during Human-to-Human Transmission of SARS-CoV-2

- Intra-host Variation and Evolutionary Dynamics of SARS-CoV-2 Population in COVID-19 Patients

- Large-scale population analysis of SARS-CoV-2 whole genome sequences reveals host-mediated viral evolution with emergence of mutations in the viral Spike protein associated with elevated mortality rates

- Genomic Diversity of Severe Acute Respiratory Syndrome-Coronavirus 2 in Patients With Coronavirus Disease 2019.

- Transmission dynamics of SARS-CoV-2 within-host diversity in two major hospital outbreaks in South Africa

Share this paper:

Population Bottlenecks and Intra-host Evolution during Human-to-Human Transmission of SARS-CoV-2

Daxi Wang[1,3#], Yanqun Wang[2#], Wanying Sun[1,3,4#], Lu Zhang[2,5#], Jingkai Ji[1,3#], Zhaoyong Zhang[2#], Xinyi Cheng[1,3,13#], Yimin Li[2#], Fei Xiao[6], Airu Zhu[2], Bei Zhong[7], Shicong Ruan[8], Jiandong Li[1,3,4], Peidi Ren[1,3], Zhihua Ou[1,3], Minfeng Xiao[1,3], Min Li[1,3,4], Ziqing Deng[1,3], Huanzi Zhong[1,3,9], Fuqiang Li[1,3,10], Wen-jing Wang[1,10], Yongwei Zhang[1], Weijun Chen[4,11], Shida Zhu[1,12], Xun Xu[1,14], Xin Jin[1], Jingxian Zhao[2], Nanshan Zhong[2], Wenwei Zhang[1*], Jincun Zhao[2,5*], Junhua Li[1,3,13*], Yonghao Xu[2*]

[1]BGI-Shenzhen, Shenzhen, 518083, China.

[2]State Key Laboratory of Respiratory Disease, National Clinical Research Center for Respiratory Disease, Guangzhou Institute of Respiratory Health, the First Affiliated Hospital of Guangzhou Medical University, Guangzhou, Guangdong, 510120, China.

[3]Shenzhen Key Laboratory of Unknown Pathogen Identification, BGI-Shenzhen, Shenzhen, 518083, China.

[4]BGI Education Center, University of Chinese Academy of Sciences, Shenzhen, 518083, China.

[5]Institute of Infectious disease, Guangzhou Eighth People's Hospital of Guangzhou Medical University, Guangzhou, Guangdong, 510060, China.

[6]Department of Infectious Diseases, Guangdong Provincial Key Laboratory of Biomedical Imaging, Guangdong Provincial Engineering Research Center of Molecular Imaging, The Fifth Affiliated Hospital, Sun Yat-sen University, Zhuhai, Guangdong, 519000, China.

[7]The Sixth Affiliated Hospital of Guangzhou Medical University, Qingyuan People's Hospital, Qingyuan, Guangdong, China.

[8]Yangjiang People's Hospital, Yangjiang, Guangdong, China

[9]Laboratory of Genomics and Molecular Biomedicine, Department of Biology, University of Copenhagen, 2100 Copenhagen, Denmark.

[10]Guangdong Provincial Key Laboratory of Human Disease Genomics, Shenzhen Key Laboratory of Genomics, BGI-Shenzhen, Shenzhen, 518083, China.

30[11]BGI PathoGenesis Pharmaceutical Technology, BGI-Shenzhen, Shenzhen, 518083, China.

31[12]Shenzhen Engineering Laboratory for Innovative Molecular Diagnostics, BGI-Shenzhen, Shenzhen,

32518120, China.

33[13]School of Biology and Biological Engineering, South China University of Technology, Guangzhou,

34China.

35[14]Guangdong Provincial Key Laboratory of Genome Read and Write, BGI-Shenzhen, Shenzhen,

36518120, China.

37[#]These authors contributed equally to this work.

38[*]These authors are corresponding authors.

39Email address: zhangww@genomics.cn

40Email address: zhaojincun@gird.cn

41Email address: lijunhua@genomics.cn

42Email address: dryonghao@163.com

43

2

44 Abstract

45 The emergence of the novel human coronavirus, SARS-CoV-2, causes a global COVID-19 46 (coronavirus disease 2019) pandemic. Here, we have characterized and compared viral populations 47 of SARS-CoV-2 among COVID-19 patients within and across households. Our work showed an active 48 viral replication activity in the human respiratory tract and the co-existence of genetically distinct 49 viruses within the same host. The inter-host comparison among viral populations further revealed a 50 narrow transmission bottleneck between patients from the same households, suggesting a dominated 51 role of stochastic dynamics in both inter-host and intra-host evolutions.

52

53 Author summary

54 In this study, we compared SARS-CoV-2 populations of 13 Chinese COVID-19 patients. Those viral 55 populations contained a considerable proportion of viral sub-genomic messenger RNAs (sgmRNA), 56 reflecting an active viral replication activity in the respiratory tract tissues. The comparison of 66 57 identified intra-host variants further showed a low viral genetic distance between intra-household 58 patients and a narrow transmission bottleneck size. Despite the co-existence of genetically distinct 59 viruses within the same host, most intra-host minor variants were not shared between transmission 60 pairs, suggesting a dominated role of stochastic dynamics in both inter-host and intra-host evolutions. 61 Furthermore, the narrow bottleneck and active viral activity in the respiratory tract show that the 62 passage of a small number of virions can cause infection. Our data have therefore delivered a key 63 genomic resource for the SARS-CoV-2 transmission research and enhanced our understanding of the 64 evolutionary dynamics of SARS-CoV-2.

65

66 Introduction

67 The rapid spread of the novel human coronavirus, SARS-CoV-2, has been causing millions of COVID-68 19 (coronavirus disease 2019) cases with high mortality rate worldwide [1,2]. As an RNA virus, SARS-69 CoV-2 mutates frequently due to the lack of sufficient mismatch repairing mechanisms during genome 70 replication [3], leading to the development of genetically different viruses within the same host. 71 Several studies have reported intra-host single nucleotide variants (iSNVs) in SARS-CoV-2 [4–6]. 72 Recently, we investigated the intra-host evolution of SARS-CoV-2 and revealed genetic differentiation 73 among tissue-specific populations [7]. However, it is still not clear how the intra-host variants circulate

3

74 among individuals. Here, we described and compared viral populations of SARS-CoV-2 among

75 COVID-19 patients within and across households. Our work here demonstrated the utilization of viral

76 genomic information to identify transmission linkage of this virus.

77

78 **Results and discussion**

79 Using both metatranscriptomic and hybrid-capture based techniques, we newly deep sequenced

80 respiratory tract (RT) samples of seven COVID-19 patients in Guangdong, China, including two pairs

81 of patients from the same households, respectively (P03 and P11; P23 and P24). The data were then

82 combined with those of 23 RT samples used in our previous study [7], yielding a combined data set of

83 30 RT samples from 13 COVID-19 patients (**Table S1**).

84   A sustained viral population should be supported by an active viral replication [8]. We firstly

85 estimated the viral transcription activity within RT samples using viral sub-genomic messenger RNAs

86 (**sgmRNAs**), which is only synthesised in infected host cells [9]. The sgmRNA abundance was

87 measured as the ratio of short reads spanning the transcription regulatory sequence (TRS) sites to

88 the viral genomic reads. The sgmRNA abundance within nasal and throat swab samples was similar

89 to that within sputum samples (**Figure 1a**), reflecting an active viral replication in the upper respiratory

90 tract. Notably, the patient P01, who eventually passed away due to COVID-19, showed the highest

91 level of sgmRNA abundance (**Figure S1**). Among the samples from patients with improved clinical

92 outcomes, their viral Ct (cycle threshold) value of reverse transcriptase quantitative PCR (RT-qPCR)

93 negatively correlated with the days post symptoms onset (**Figure 1b**). Interestingly, the sgmRNA

94 abundance showed a similar trend across time (**Figure 1c**). This result is further strengthened by the

95 positive correlation between sgmRNA abundance and the Ct value (**Figure 1d**), reflecting a direct

96 biological association between viral replication and viral shedding in the respiratory tract tissues.

97   Using the metatranscriptomic data, we identified 66 iSNVs in protein encoding regions with the

98 alternative allele frequency (AAF) ranged from 5% to 95% (**Table S2 and Table S3**). The identified

99 iSNVs showed a high concordance between the AAFs derived from metatranscriptomic and that from

100 hybrid-capture sequences (Spearman's ρ = 0.81, P < 2.2e-16; **Figure S2**). We firstly looked for

101 signals of natural selection against intra-host variants. Using the Fisher's exact test, we compared the

102 number of iSNV sites on each codon position against that of the other two positions and detected a

103 significant difference among them (codon position 1[n = 10, P = 0.02], 2 [n = 21; P = 1] and 3 [n = 35;

4

104 P = 0.03]). However, those iSNVs did not show a discriminated AAF among the non-synonymous and

105 synonymous categories (**Figure 2a**), suggesting that most non-synonymous variants were not under

106 an effective purifying selection within the host. Among the 66 identified iSNVs, 30 were coincided with

107 the consensus variants in the public database (**Table S2**). Those iSNVs were categorised into

108 common iSNVs, while the iSNVs presented in a single patient were categorised into rare iSNVs.

109 Interestingly, the common iSNVs had a significant higher minor allele frequency compared to the rare

110 iSNVs (**Figure S3;** Wilcoxon rank sum test, P = 2.7e-05), suggesting that they may have been

111 developed in earlier strains before the most recent infection.

112   We then estimated the viral genetic distance among samples in a pairwise manner based on their

113 iSNVs and allele frequencies. The samples were firstly categorised into intra-host pairs (serial

114 samples from the same host), intra-household pairs and inter-household pairs (**Figure 2b and Table**

115 **S4**). As expected, the intra-host pairs had the lowest genetic distance compared to either intra-

116 household pairs (Wilcoxon rank sum test, P = 0.018) and inter-household pairs (Wilcoxon rank sum

117 test, P < 2.22e-16). Interestingly, the genetic distance between intra-household pairs was significantly

118 lower than that of inter-household pairs (**Figure 2b;** Wilcoxon rank sum test, P = 0.03), supporting a

119 direct passage of virions among intra-household individuals. Nonetheless, we only observed a few

120 minor variants shared among intra-household pairs, suggesting that the estimated genetic similarity

121 was mostly determined by consensus nucleotide differences (**Figure 2c,d**). Specifically, in one intra-

122 household pair (P23 and P24), one patient (P23) contained iSNVs that were coincided with the linked

123 variants, C8782T and T28144C, suggesting that this patient may have been co-infected by genetically

124 distinct viruses. However, the strain carrying C8782T and T28144C was not observed in the intra-

125 household counterpart (P24). It is likely that there is a narrow transmission bottleneck allowing only

126 the major strain to be circulated, if P23 was infected by all the observed viral strains before the

127 transmission.

128   The transmission bottlenecks among intra-household pairs were estimated using a beta binomial

129 model, which was designed to allow some temporal stochastic dynamics of viral population in the

130 recipient [10]. Here, we defined the donor and recipient within the intra-household pairs according to

131 their dates of the first symptom onset. The estimated bottleneck sizes were 6 (P03 and P11) and 8

132 (P23 and P24) for the two intra-household pairs (**Table S5**). This result is consistent with the patterns

133 observed in many animal viruses and human respiratory viruses [11,12], while the only study reporting

134 a loose bottleneck among human respiratory viral infections [13] was argued as the generic

135 consequence of shared iSNVs caused by read mapping artefacts [14]. The relatively narrow

136 transmission bottleneck sizes is expected to increase the variance of viral variants being circulated

137 between transmission pairs [15]. Even after successful transmission, virions carrying the minor

138 variants are likely to be purged out due to the frequent stochastic dynamics within the respiratory tract

139 [7], which is also consistent with the low diversity and instable iSNV observed among the RT samples.

140   The observed narrow transmission bottleneck suggests that, in general, only a few virions

141 successfully enter host cells and eventually cause infection. Although the number of transmitted

142 virions is sparse, they can easily replicate in the respiratory tract, given the observed viral replication

143 activities in all the RT sample types and the high host-cell receptor binding affinity of SARS-CoV-2

144 [16]. The narrow transmission bottleneck also indicate that instant hand hygiene and mask-wearing

145 might be particular effective in blocking the transmission chain of SARS-CoV-2.

146   In summary, we have characterized and compared SARS-CoV-2 populations of patients within and

147 across households using both metatranscriptomic and hybrid-capture based techniques. Our work

148 showed an active viral replication activity in the human respiratory tract and the co-existence of

149 genetically distinct viruses within the same host. The inter-host comparison among viral populations

150 further revealed a narrow transmission bottleneck between patients from the same households,

151 suggesting a dominated role of stochastic dynamics in both inter-host and intra-host evolution. The

152 present work enhanced our understanding of SARS-CoV-2 virus transmission and shed light on the

153 integration of genomic and epidemiological in the control of this virus.

6

Materials and methods

Patient and Ethics statement

Respiratory tract (RT) samples, including nasal swabs, throat swabs, sputum, were collected from 13 COVID-19 patients during the early outbreak of the pandemic (from January 25 to February 10 of 2020). Those patients were hospitalized at the first affiliated hospital of Guangzhou Medical University (10 patients), the fifth affiliated hospital of Sun Yat-sen University (1 patient), Qingyuan People's Hospital (1 patient) and Yangjiang People's Hospital (1 patient). The research plan was assessed and approved by the Ethics Committee of each hospital. All the privacy information was anonymized.

Dataset description

Public consensus sequences were downloaded from GISAID.

Real-time RT-qPCR and sequencing

RNA was extracted from the clinical RT samples using QIAamp Viral RNA Mini Kit (Qiagen, Hilden, Germany), which was then tested for SARS-CoV-2 using Real-time RT-qPCR. Human DNA was removed using DNase I and RNA concentration was measured using Qubit RNA HS Assay Kit (Thermo Fisher Scientific, Waltham, MA, USA). After human DNA-depletion, the samples were RNA purified and then subjected to double-stranded DNA library construction using the MGIEasy RNA Library preparation reagent set (MGI, Shenzhen, China) following the method used in the previous study [17]. Possible contamination during experimental processing was tracked using human breast cell lines (Michigan Cancer Foundation-7). The constructed libraries were converted to DNA nanoballs (DNBs) and then sequenced on the DNBSEQ-T7 platform (MGI, Shenzhen, China), generating paired-end short reads with 100bp in length. Most samples were also sequenced using hybrid capture-based enrichment approach that was described in previous study [17]. Briefly, the SARS-CoV-2 genomic content was enriched from the double-stranded DNA libraries using the 2019-nCoVirus DNA/RNA Capture Panel (BOKE, Jiangsu, China). The enriched SARS-CoV-2 genomic contents were converted to DNBs and then sequenced on the MGISEQ-2000 platform, generating paired-end short reads with 100bp in length.

7

183 **Data filtering**

184 Read data from both metatranscriptomic and hybrid capture based sequencing were filtered following 185 the steps described in the previous research [17]. In brief, short read data were mapped to a database 186 that contains major coronaviridae genomes. Low-quality, adaptor contaminations, duplications, and 187 low-complexity within the mapped reads were removed to generate the high quality coronaviridae-like 188 short read data.

189

190 **Profiling of sub-genomic messenger RNA (sgmRNAs)**

191 Coronaviridae-like short reads were mapped to the reference genome (EPI_ISL_402119) using the 192 aligner HISAT2 [18]. Reads spanning the transcription regulatory sequence (TRS) sites of both leader 193 region and the coding genes (S gene, ORF3a, 6, 7a, 8, E, M and N gene) were selected to represent 194 the sgmRNAs. The junction sites were predicted using RegTools junctions extract [19]. The ratio of 195 sgmRNA reads to the viral genomic RNA reads (sgmRNA ratio) was used to estimate the relative 196 transcription activity of SARS-CoV-2.

197

198 **Detection of intra-host variants**

199 We defined an intra-host single nucleotide variant (iSNV) as the co-existence of an alternative allele 200 and the reference allele at the same genomic position within the same sample. To identify iSNV sites, 201 paired-end metatranscriptomic coronaviridae-like short read data were mapped to the reference 202 genome (EPI_ISL_402119) using BWA aln (v.0.7.16) with default parameters [20]. The duplicated 203 reads were detected and marked using Picard MarkDuplicates (v. 2.10.10) 204 (http://broadinstitute.github.io/picard). Nucleotide composition of each genomic position was 205 characterized from the read mapping results using pysamstats (v. 1.1.2) 206 (https://github.com/alimanfoo/pysamstats). The variable sites of each sample were identified using the 207 variant caller LoFreq with default filters and the cut-off of 5% minor allele frequency. After filtering the 208 sites with more than one alternative allele, the rest sites were regarded as iSNV sites. All the iSNVs 209 with less than five metatranscriptomic reads were verified using the hybrid capture data (at least two 210 reads). The identified iSNVs were then annotated using the SnpEff (v.2.0.5) with default settings [21].

211

8

212**Genetic distance**

213The genetic distance between sample pairs was calculated using L1-norm distance, as defined by the

214following formula. The L1-norm distance (D) between sample pairs is calculated by summing the

215distance of all the variable loci (N). The distance on each variable locus is calculated between vectors

216(p and q for each sample) of possible base frequencies ($n=4$¿.

217$$D=\sum_{k=1}^{N}\sum_{i=1}^{n} ¿p_i-q_i \vee ¿¿$$

218To verify the result, L2-norm distance (Euclidean distance) between sample pairs was calculated. The

219L2-norm distance $d(p,q)$ between two samples (p,q) is the square root of sum of distance across

220all the variable loci (N), as defined by the following formula.

221$$d(p,q)=\sqrt{\sum_{i=1}^{n}(p_i-q_i)^2}$$

222The comparison of genetic distances among sample pair categories was performed using the

223Wilcoxon rank-sum test.

224

225**Beta binomial model of bottleneck size estimation**

226A beta-binomial model was used to estimate bottleneck sizes between donors and recipients. Here,

227the bottleneck size represents the number of virions that pass into the recipient and finally shape the

228sequenced viral population. The patient with the earlier symptom onset date was defined as the

229donor, while the other was defined as the recipient. The maximum-likelihood estimates (MLE) of

230bottleneck sizes were estimated within 95% confidence intervals.

9

References

1. Wu F, Zhao S, Yu B, Chen YM, Wang W, Song ZG, et al. A new coronavirus associated with human respiratory disease in China. Nature. 2020. doi:10.1038/s41586-020-2008-3

2. Zhou P, Yang X Lou, Wang XG, Hu B, Zhang L, Zhang W, et al. A pneumonia outbreak associated with a new coronavirus of probable bat origin. Nature. 2020. doi:10.1038/s41586-020-2012-7

3. Smith EC, Sexton NR, Denison MR. Thinking Outside the Triangle: Replication Fidelity of the Largest RNA Viruses. Annu Rev Virol. 2014;1: 111–132. doi:10.1146/annurev-virology-031413-085507

4. Shen Z. Genomic diversity of SARS-CoV-2 in Coronavirus Disease 2019 patients. bioRvix. 2019; 1–27.

5. Butler DJ, Mozsary C, Meydan C, Danko D, Foox J, Rosiene J, et al. Shotgun Transcriptome and Isothermal Profiling of SARS-CoV-2 Infection Reveals Unique Host Responses, Viral Diversification, and Drug Interactions. bioRxiv. 2020. doi:10.1101/2020.04.20.048066

6. Fraser C, Crook D, Peto T, Andersson M, Jeffries K, Eyre D, et al. Shared SARS-CoV-2 diversity suggests localised transmission of minority variants. 2020.

7. Wang Y, Wang D, Zhang L, Sun W, Zhang Z, Chen W, et al. Intra-host Variation and Evolutionary Dynamics of SARS-CoV-2 Population in COVID-19 Patients. bioRxiv. 2020. doi:10.1101/2020.05.20.103549

8. Wölfel R, Corman VM, Guggemos W, Seilmaier M, Zange S, Müller MA, et al. Virological assessment of hospitalized patients with COVID-2019. Nature. 2020. doi:10.1038/s41586-020-2196-x

9. Sola I, Almazán F, Zúñiga S, Enjuanes L. Continuous and Discontinuous RNA Synthesis in Coronaviruses. Annu Rev Virol. 2015;2: 265–288. doi:10.1146/annurev-virology-100114-055218

10. Sobel Leonard A, Weissman DB, Greenbaum B, Ghedin E, Koelle K. Transmission Bottleneck Size Estimation from Pathogen Deep-Sequencing Data, with an Application to Human Influenza A Virus. J Virol. 2017;91: 0–19. doi:10.1128/jvi.00171-17

11. Zwart MP, Elena SF. Matters of Size: Genetic Bottlenecks in Virus Infection and Their Potential Impact on Evolution. Annu Rev Virol. 2015;2: 161–179. doi:10.1146/annurev-

10

261   virology-100114-055135

262 12.   McCrone JT, Woods RJ, Martin ET, Malosh RE, Monto AS, Lauring AS. Stochastic processes constrain the within and between host evolution of influenza virus. Elife. 2018;7: 1–19. doi:10.7554/eLife.35962

265 13.   Poon LLM, Song T, Rosenfeld R, Lin X, Rogers MB, Zhou B, et al. Quantifying influenza virus diversity and transmission in humans. Nat Genet. 2016;48: 195–200. doi:10.1038/ng.3479

267 14.   Xue KS, Bloom JD. Reconciling disparate estimates of viral genetic diversity during human influenza infections. Nat Genet. 2019;51: 1298–1301. doi:10.1038/s41588-019-0349-3

269 15.   Xue KS, Moncla LH, Bedford T, Bloom JD. Within-Host Evolution of Human Influenza Virus. Trends Microbiol. 2018;26: 781–793. doi:10.1016/j.tim.2018.02.007

271 16.   Shang J, Ye G, Shi K, Wan Y, Luo C, Aihara H, et al. Structural basis of receptor recognition by SARS-CoV-2. Nature. 2020. doi:10.1038/s41586-020-2179-y

273 17.   Xiao M, Liu X, Ji J, Li M, Li J, Sun W, et al. Multiple approaches for massively parallel sequencing of HCoV-19 genomes directly from clinical samples 2. 2020; 33. doi:10.1101/2020.03.16.993584

276 18.   Kim D, Langmead B, Salzberg SL. HISAT: A fast spliced aligner with low memory requirements. Nat Methods. 2015. doi:10.1038/nmeth.3317

278 19.   Feng Y-Y, Ramu A, Cotto KC, Skidmore ZL, Kunisaki J, Conrad DF, et al. RegTools: Integrated analysis of genomic and transcriptomic data for discovery of splicing variants in cancer. bioRxiv. 2018. doi:10.1101/436634

281 20.   Li H, Durbin R. Fast and accurate long-read alignment with Burrows-Wheeler transform. Bioinformatics. 2010. doi:10.1093/bioinformatics/btp698

283 21.   Cingolani P, Platts A, Wang LL, Coon M, Nguyen T, Wang L, et al. A program for annotating and predicting the effects of single nucleotide polymorphisms, SnpEff. Fly (Austin). 2012. doi:10.4161/fly.19695

286

11

287 DATA AVAILABILITY

288 The data that support the findings of this study have been deposited into CNSA (CNGB Sequence

289 Archive) of CNGBdb with the accession number CNP0001111 (https://db.cngb.org/cnsa/).

290

291 DISCLOSURE STATEMENT

292 No conflict of interest was reported by the authors

293

294 ACKNOWLEDGEMENTS

307

308 AUTHOR CONTRIBUTIONS

309 D.W., Y.X., J.L., W.Z. and J.Z. conceived the study, Y.W., L.Z., and Y.L. collected clinical specimen
310 and executed the experiments. D.W., W.S., X.C. and J.J. analyzed the data. All the authors
311 participated in discussion and result interpretation. D.W., Y.W., and Z.Z. wrote the manuscript. All
312 authors revised and approved the final version.

12

313 **Figures**
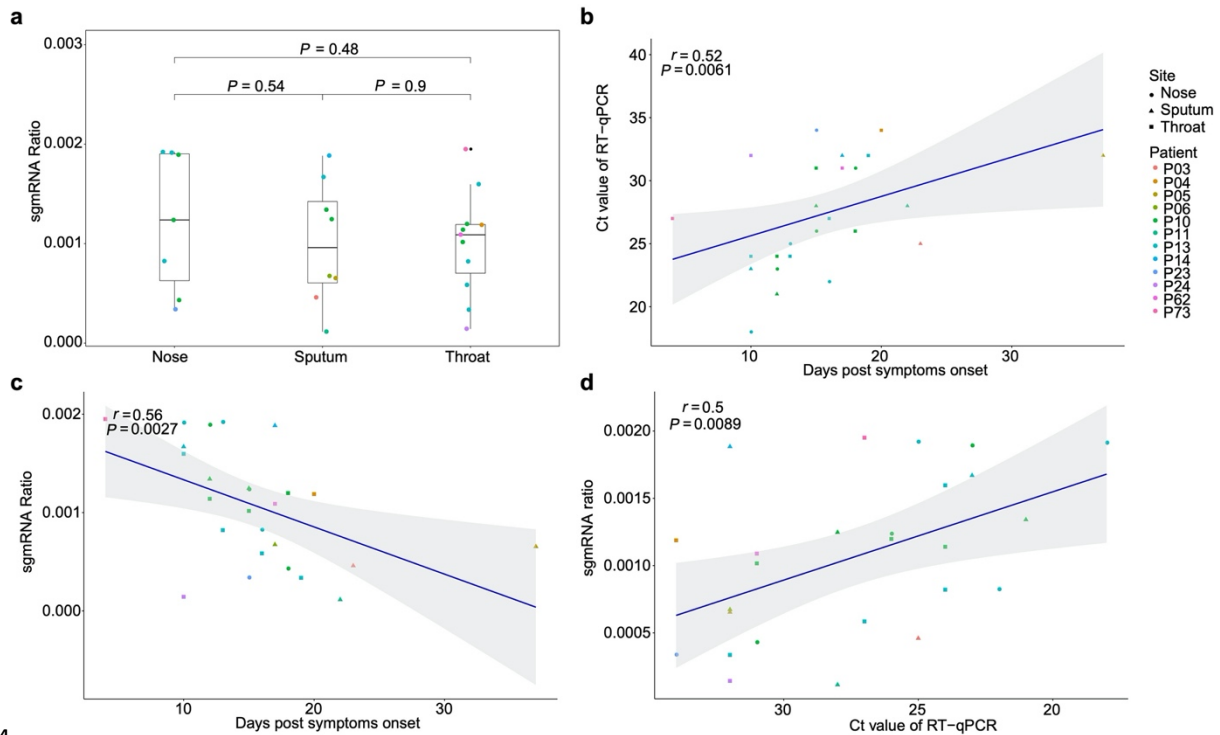
314

315 **Figure 1. sub-genomic messenger RNAs (sgmRNAs)**

316 **a,** The ratio of sgmRNA of each respiratory sample type (nasal, throat swabs and sputum). **b,**

317 Correlation between the cycle threshold (Ct) of RT-qPCR and the days post symptoms onset. **c,**

318 Correlation between estimated sgmRNA ratio and the days post symtoms onset. **d,** Correlation

319 between estimated sgmRNA ratio and the cycle threshold of RT-qPCR.

13

320
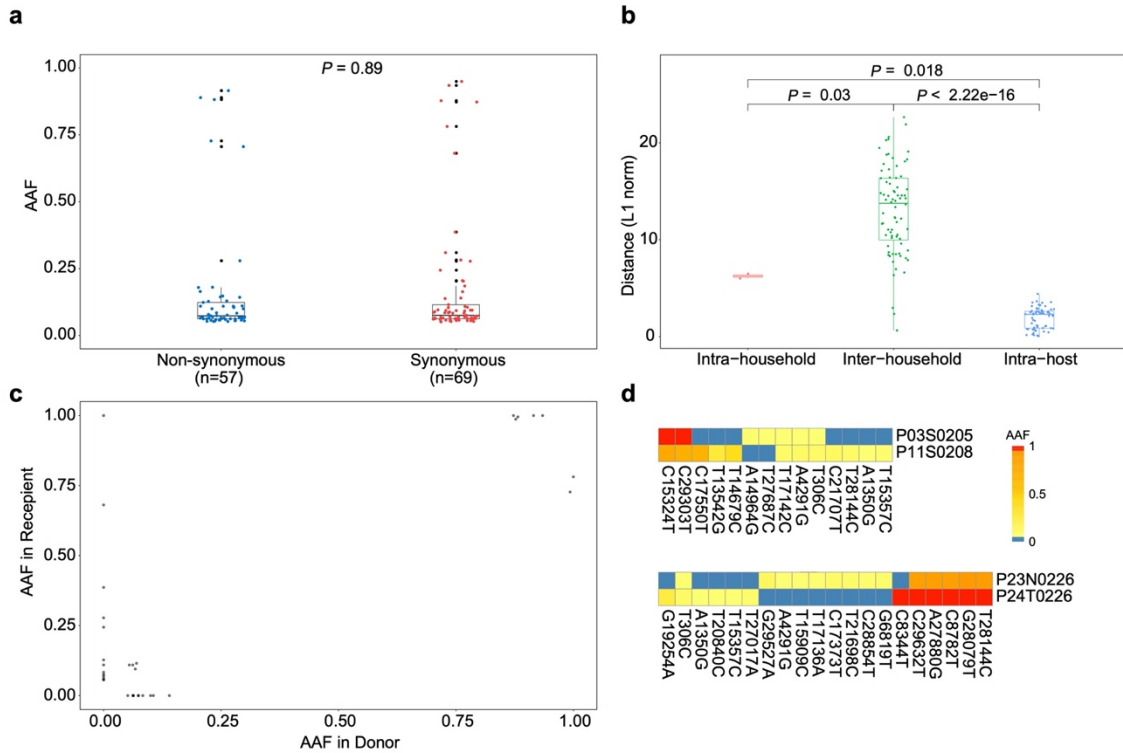
Figure 2. Allele frequency changes of transmission pairs

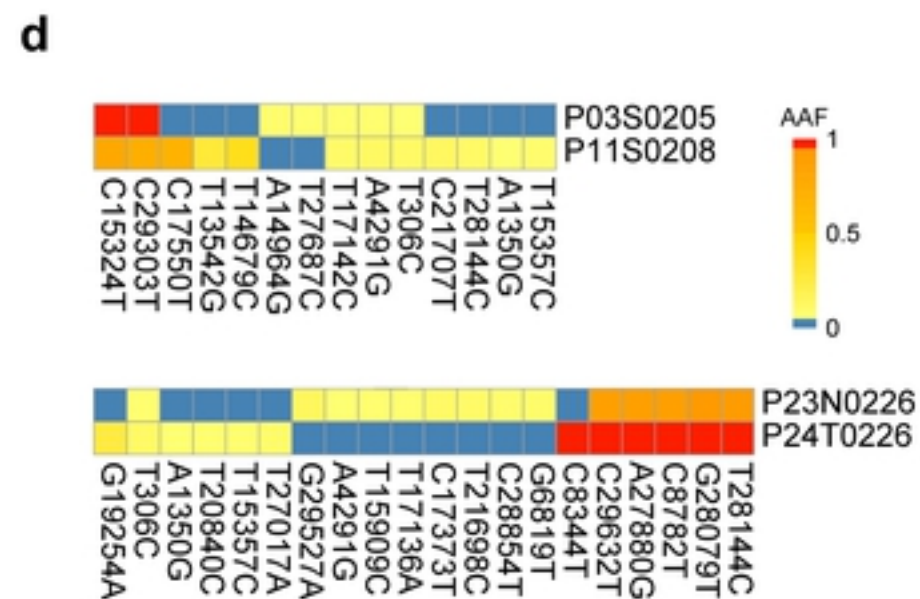**a,** Box plots showing the alternative allele frequency (AAF) distribution of synonymous and non-synonymous intra-host variants. **b,** Box plots representing the L1-norm distance distribution among sample pairs. Each dot represents the genetic distance between each sample pair. **c,** The AAF of donor iSNVs in transmission pairs. Allele frequencies under 5% and over 95% were adjusted to 0% and 1, respectively. **d,** Heatmap representing the alternative allele frequencies (AAFs) of consensus and intra-host single nucleotide variants (iSNVs) of the two transmission pairs.

14

328**SUPPLEMENTARY INFORMATION**

329**Table S1. Demography and clinical outcomes of COVID-19 patients**

330**Table S2. Summary of iSNVs**

331**Table S3. Frequency of iSNVs**

332**Table S4. Inter-host genetic distance (L1 and L2-norm)**

333**Table S5. Bottleneck size of intra-household pairs**

334

15
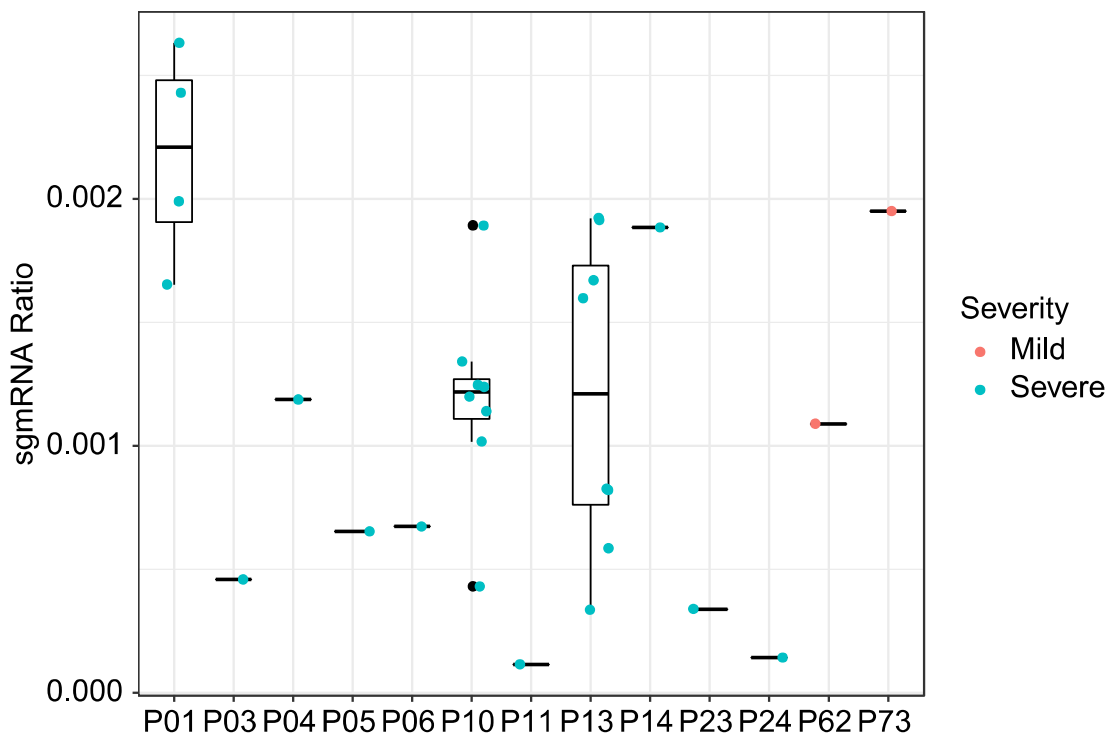
Figure S1. Transcription profile of sub-genomic messenger RNAs (sgmRNAs) of each patient.

16

338
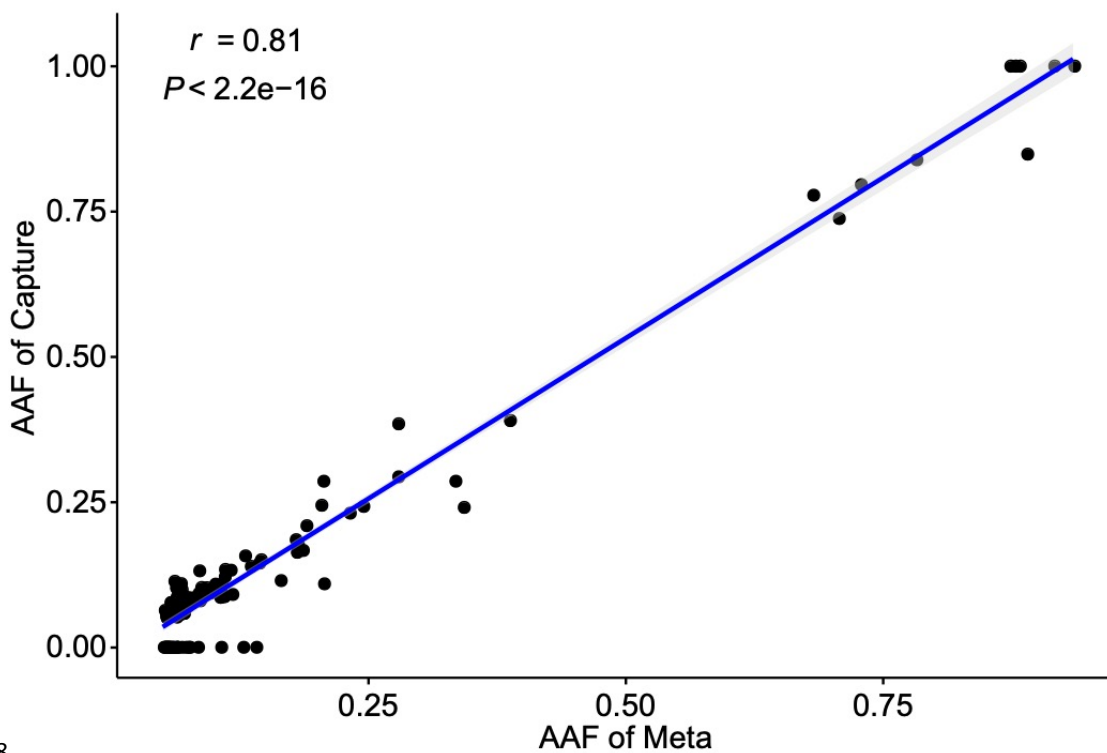
Figure S2. Concordance between minor alternative allele frequencies (AAFs) derived from metagenomic and hybrid capture data.

341

17
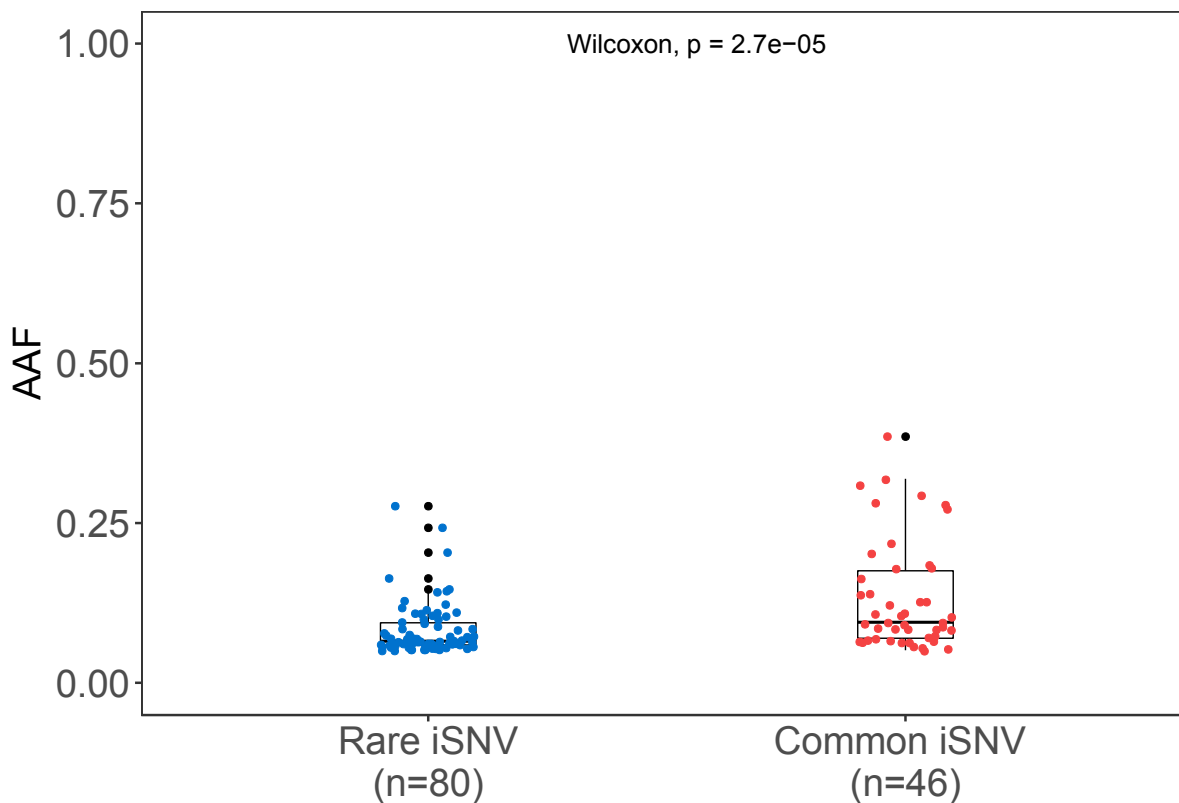
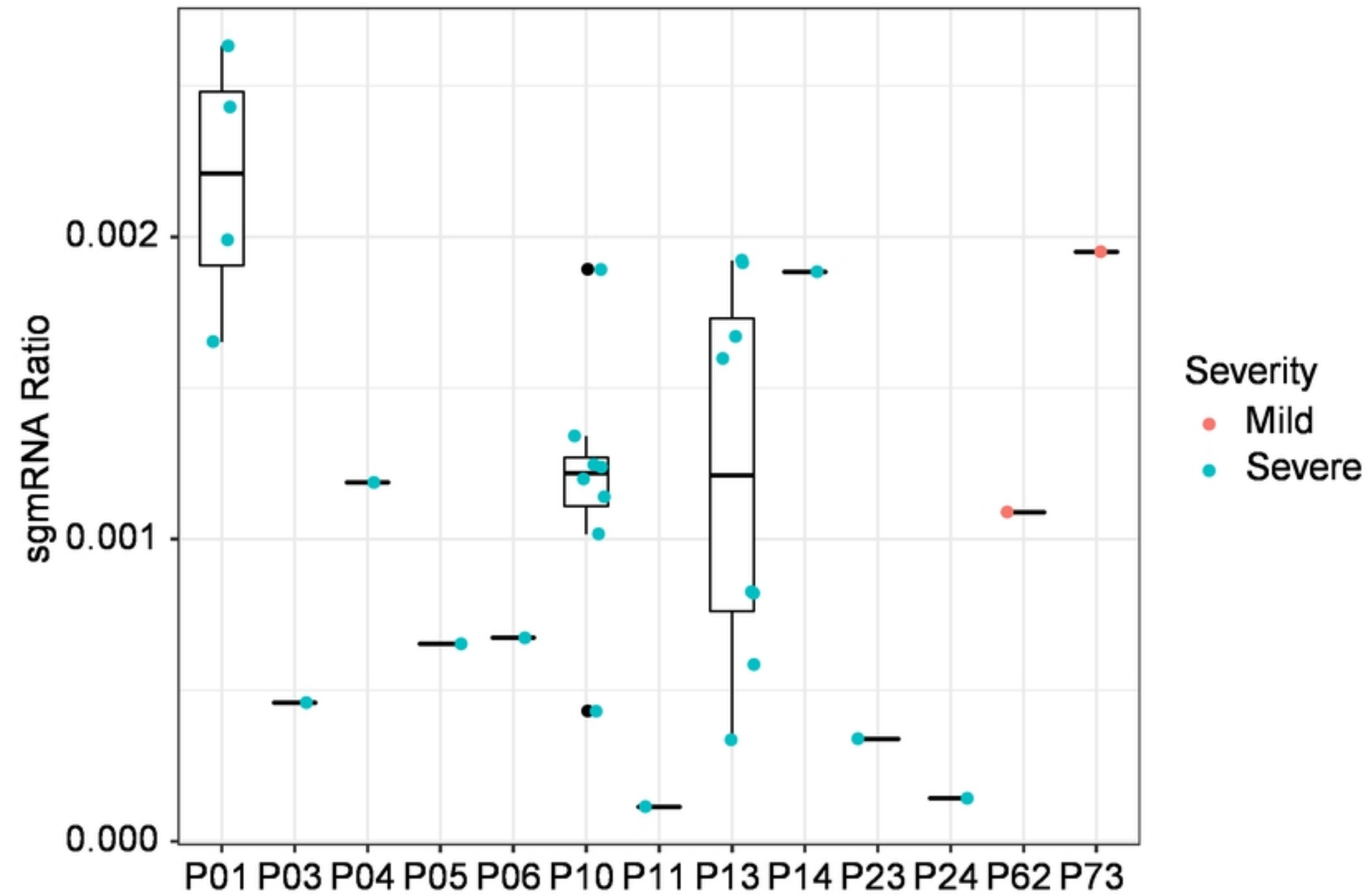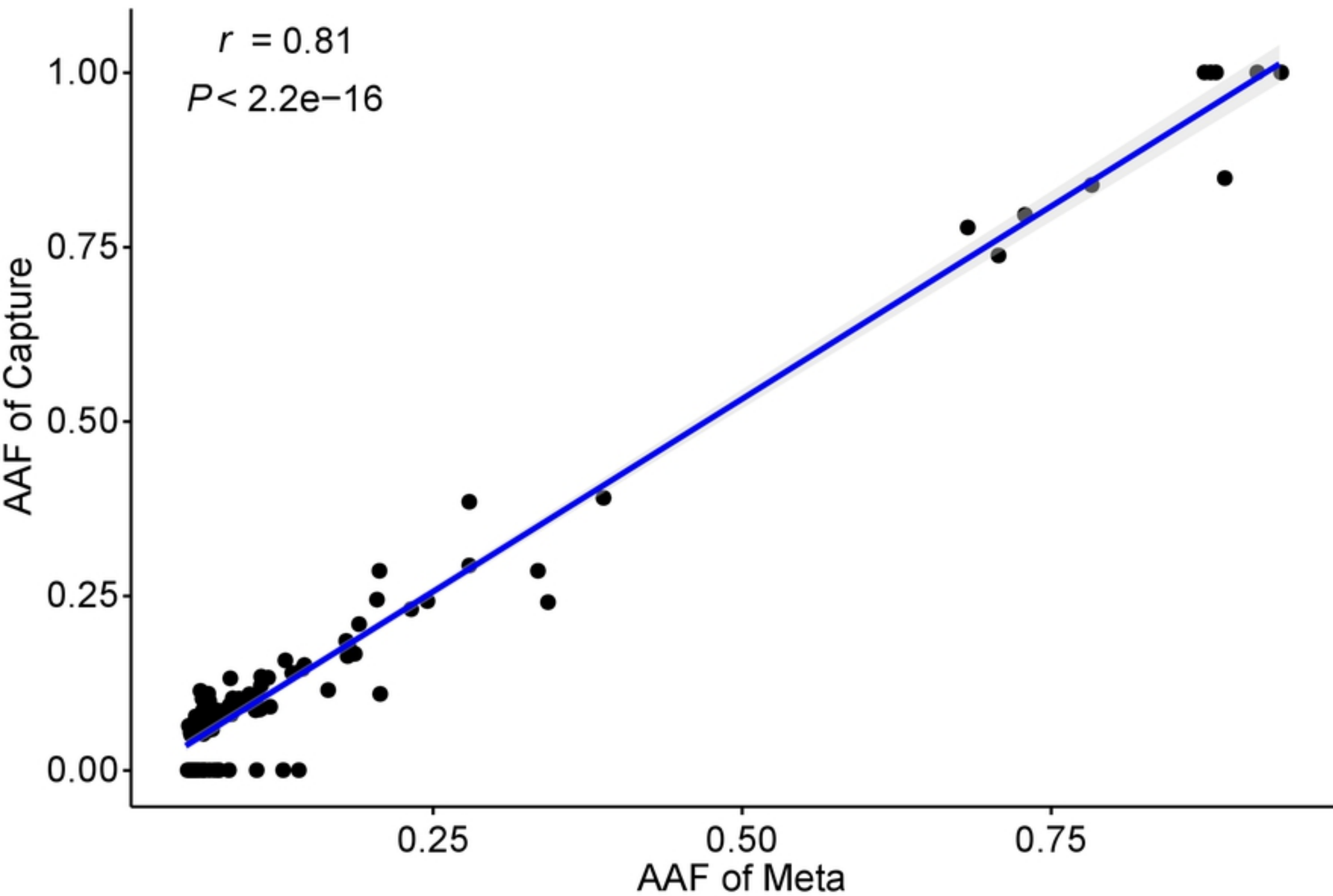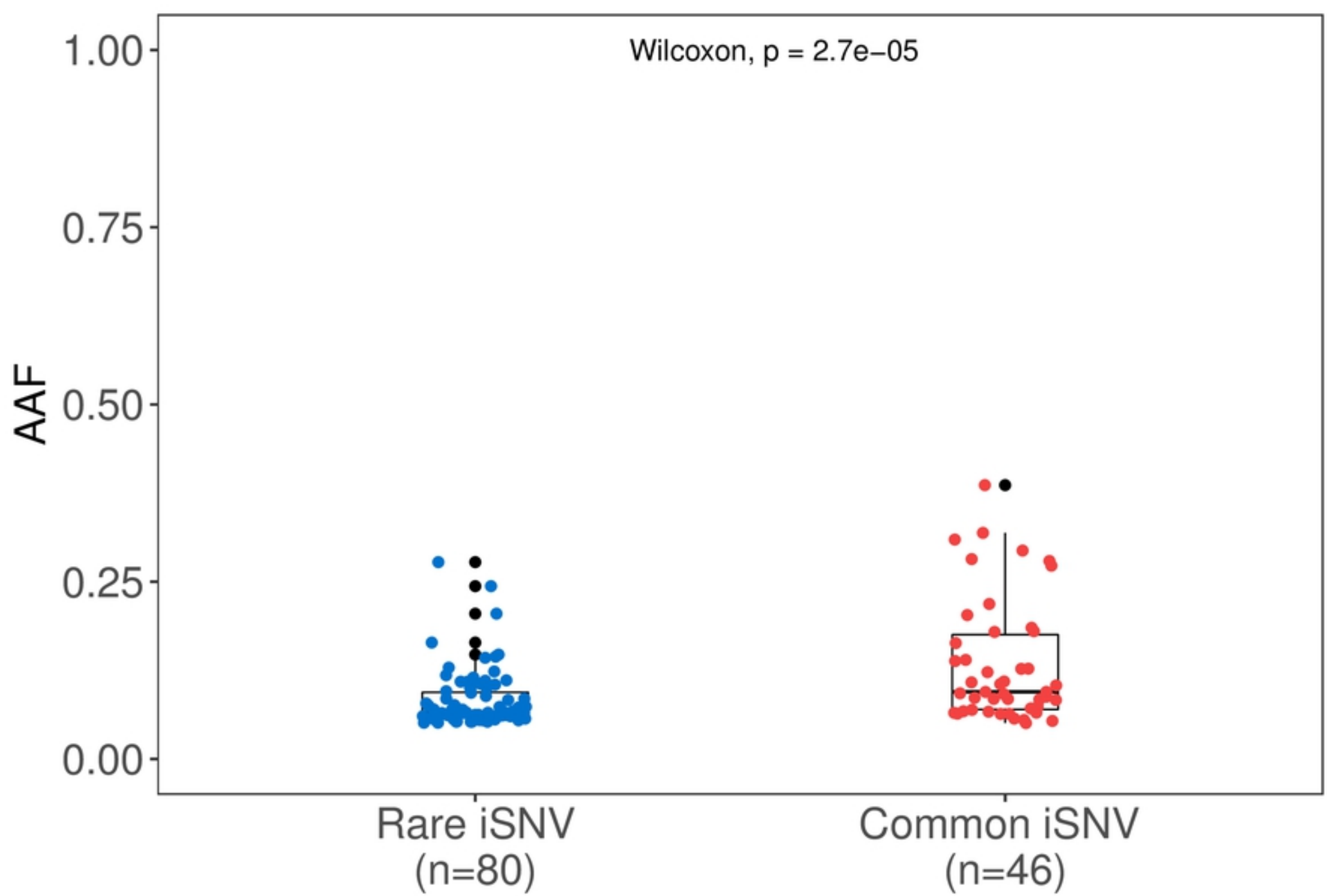342 **Figure S3. Alternative allele frequency (AAF) distribution of rare and common iSNVs**

343

18

Figure

Figure

Figure

Figure

Figure